Available online at www.sciencedirect.com
SCIENCE DIRECT
Journal of Sound and Vibration 294 (2006) 663–677
JOURNAL OF SOUND AND VIBRATION
www.elsevier.com/locate/jsvi

Resonance vibrations of an elastic interfacial layer

J. Kaplunov*, A. Krynkin

Department of Mathematics, The University of Manchester, Manchester M13 9PL, UK

Received 23 December 2004; received in revised form 21 November 2005; accepted 29 November 2005
Available online 9 March 2006

Abstract

Resonance interfacial phenomena are studied in relation to forced plane vibrations of an elastic layer enclosed between two half-spaces. Complex thickness resonance frequencies are examined for the system in question. An asymptotic approach is developed to analyse "soft" and "hard" interfaces. The applicability of high-frequency long-wavelength one-dimensional models is justified for describing thickness vibrations of a radiating interfacial layer. Numerical results are presented that illustrate the efficiency of the proposed asymptotic expansions by comparing with the exact solution which is expressed in terms of Fourier integrals.

1. Introduction

The theory of wave propagation in layered media is a classical sub-area of continuum mechanics and acoustics (see Refs. [1–4] and references therein). In the framework of this theory, the dynamic analysis of elastic interfaces is of interest for many modern applications, including composite technology and geotechnical engineering. Many of the publications on the subject are motivated by non-destructive evaluation for structural elements, in particular, for adhesive joints (e.g. see Refs. [5–8]).

Our main aim is to obtain a deeper qualitative insight into resonance interfacial phenomena. The specific goal is to consider forced vibrations of "hard/soft" interfacial layers characterising by small/large wave impedances related to that of the environment (see formula (1) below). Since the degenerate model of a single layer with traction free or fixed faces ignores the loss of vibration energy caused by the radiation into the environment, we expect a near-resonance behaviour of a "hard" and "soft" layer that generates only a small radiation.

For elongated interfaces, the so-called thickness vibrations correspond to the only type of resonance excitation. These vibrations are associated with one-dimensional (1D) eigenmodes of an infinitesimal transverse fibre and are characterised by wavelengths along the interface that are greater than the layer thickness; they have been investigated in a great detail for thin elastic plates and shells (e.g. see Refs. [3,9,10]).

To fix ideas we adopt a simple model plane problem in elasticity which is an infinite layer enclosed between two half-spaces. For the sake of definiteness, forced vibrations are assumed to be induced by two "δ-type" vertical forces applied symmetrically to the layer; the conditions of ideal elastic contact are imposed.

*Corresponding author. Present address: Department of Mathematical Sciences, Brunel University, Uxbridge, Middlesex, UB8 3PH, UK. Tel.: +44 1895 266 119.
E-mail address: Julius.Kaplunov@brunel.ac.uk (J. Kaplunov).

0022-460X/$ - see front matter
doi:10.1016/j.jsv.2005.11.030

The exact solution of this model problem is expressed in terms of Fourier integrals and an asymptotic analysis near complex thickness stretch resonance frequencies is given in Section 5. The real parts of these frequencies coincide with the limiting eigenvalues for a layer with traction free or fixed faces, whereas their imaginary parts incorporate the effect of the radiation to infinity and become small both for "hard" and "soft" interfaces. The concept of a complex resonance frequency exploited within this paper is wide spread in resonance scattering theory (e.g. see Ref. [11]).

Explicit asymptotic formulae are derived for resonance displacements and stresses based only upon the contributions of long-wavelength components in the original Fourier integrals. It is remarkable that the same formulae also follow from the 1D equations describing high-frequency long-wavelength vibrations of an elastic layer radiating into softer or harder environment. These equations govern vibration modes with a slow variation along the interface. At the same time associated frequencies are close to higher order cut-offs that coincide with so-called thickness stretch resonance frequencies. The developed approach generalises previous considerations reported in the above-mentioned papers Refs. [9,10] and the book Ref. [3]. The analysis of high-frequency forced vibrations of an elastic plate in the case of a light fluid loading in Ref. [9] is particularly relevant to the treatment below.

Numerical comparison with the exact solution demonstrates the high accuracy of the proposed asymptotic expansions over a wide range of problem parameters both for resonance curves and spatial distributions of displacements and stresses. These are especially useful for smoother loads that may suppress the considerable effect of small-amplitude short-wavelength components.

2. Statement of the problem

We consider harmonic vibrations of elastic flat layer of thickness $2h$ enclosed by an infinite homogeneous elastic continuum. Let the $x_3 = 0$ plane, in the Cartesian coordinate system (x_1, x_2, x_3), be the mid-plane of the layer with the Ox_3 axis directed into the upper half-space $x_3 \geqslant 0$ and two symmetrical "δ-type" vertical forces of amplitude A are applied to the interfaces at $x_3 = \pm h$ (see Fig. 1). In this paper, we concentrate on the 2D plane-strain problem assuming that the forces are uniformly distributed along the Ox_2 axis.

We adopt the notation: $\nu^{(i)}$ are the Poisson ratios; $\rho^{(i)}$ are the densities; $c_1^{(i)}$ and $c_2^{(i)}$ are longitudinal and transverse wave velocities, respectively (here, and below, $i = 1$ for the infinite media and $i = 2$ for the layer). We also introduce the dimensionless quantities:

$$c_* = \frac{c_2^{(1)}}{c_2^{(2)}}, \quad \rho_* = \frac{\rho^{(1)}}{\rho^{(2)}}, \quad \varepsilon = c_* \rho_*, \quad \kappa^{(i)} = \frac{c_2^{(i)}}{c_1^{(i)}} = \sqrt{\frac{1 - 2\nu^{(i)}}{2 - 2\nu^{(i)}}}, \tag{1}$$

where the parameter ε expressing the relative impedance of the layer is of particular importance.

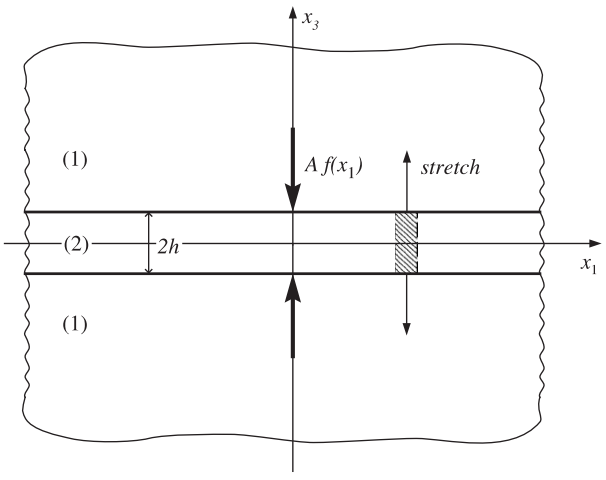

Fig. 1. Transverse symmetric loading of interfacial layer.

We define the displacements of the layer and the environment (e.g. see Ref. [12] for more details) in the form

$$v_1^{(i)}(x_1,x_3)=\frac{\partial\phi^{(i)}}{\partial x_1}-\frac{\partial\psi^{(i)}}{\partial x_3},\quad v_3^{(i)}(x_1,x_3)=\frac{\partial\phi^{(i)}}{\partial x_3}+\frac{\partial\psi^{(i)}}{\partial x_1}, \tag{2}$$

where $\phi^{(i)}(x_1,x_3)$ and $\psi^{(i)}(x_1,x_3)$ are the Lamé potentials. These potentials satisfy the Helmholtz equations

$$\Delta\phi^{(i)}+\left(\frac{\omega}{c_1^{(i)}}\right)^2\phi^{(i)}=0 \tag{3}$$

and

$$\Delta\psi^{(i)}+\left(\frac{\omega}{c_2^{(i)}}\right)^2\psi^{(i)}=0, \tag{4}$$

where ω is circular frequency (the common factor $\exp(\mathrm{i}\omega t)$ is considered understood throughout and henceforth is omitted); Δ is the plane Laplacian, i.e. $\Delta=(\partial^2/\partial x_1^2)+(\partial^2/\partial x_3^2)$.

The stresses are also expressed in the terms of these potentials $\phi^{(i)}$ and $\psi^{(i)}$, in particular,

$$\begin{aligned}\sigma_{31}^{(i)}&=(c_2^{(i)})^2\rho^{(i)}\left[\left(\frac{\omega}{c_2^{(i)}}\right)^2\psi^{(i)}+2\frac{\partial^2\phi^{(i)}}{\partial x_1\partial x_3}+2\frac{\partial^2\psi^{(i)}}{\partial x_1^2}\right],\\ \sigma_{33}^{(i)}&=(c_2^{(i)})^2\rho^{(i)}\left[-\left(\frac{\omega}{c_2^{(i)}}\right)^2\phi^{(i)}+2\frac{\partial^2\psi^{(i)}}{\partial x_1\partial x_3}-2\frac{\partial^2\phi^{(i)}}{\partial x_1^2}\right].\end{aligned} \tag{5}$$

The continuity conditions on the interfaces $x_3=\pm h$, modelling an ideal elastic contact, are written as

$$v_1^{(1)}=v_1^{(2)},\quad v_3^{(1)}=v_3^{(2)} \tag{6}$$

and

$$\sigma_{31}^{(1)}=\sigma_{31}^{(2)},\quad \sigma_{33}^{(1)}=\sigma_{33}^{(2)}+Af(x_1), \tag{7}$$

where A is a constant, the function $f(x_1)$ is a "δ-type" force and is given by

$$f(x_1)=\frac{\beta}{\pi(x_1^2+\beta^2)}, \tag{8}$$

with small β (see Fig. 2).

In addition, the Lamé potentials $\phi^{(1)}$ and $\psi^{(1)}$ have to satisfy the radiation condition at infinity. For bulk waves these are written as

$$\frac{\partial\phi^{(1)}}{\partial r}+\mathrm{i}\frac{\omega}{c_1^{(1)}}\phi^{(1)}=o\left(\frac{1}{\sqrt{r}}\right)\quad\text{and}\quad\frac{\partial\psi^{(1)}}{\partial r}+\mathrm{i}\frac{\omega}{c_2^{(1)}}\psi^{(1)}=o\left(\frac{1}{\sqrt{r}}\right), \tag{9}$$

where $r=\sqrt{x_1^2+x_3^2}$.

Our main goal is to analyse resonance phenomena specific to a "hard" or "soft" interfacial layer, when the parameter ε in Eq. (1) is small or large, respectively. In the limit $\varepsilon=0$, we arrive at a single layer with traction free faces, whereas the limit $\varepsilon\to\infty$ corresponds to a single layer with fixed faces. For both of these limiting cases, radiation into the infinite media does not occur and all the vibration energy remains within the interface.

3. Exact solution

First, we define the Fourier transform as

$$g_F(\alpha,x_3)=\int_{-\infty}^{+\infty}g(x_1,x_3)\exp\left(-\mathrm{i}\Omega\frac{x_1}{h}\alpha\right)\mathrm{d}x_1, \tag{10}$$

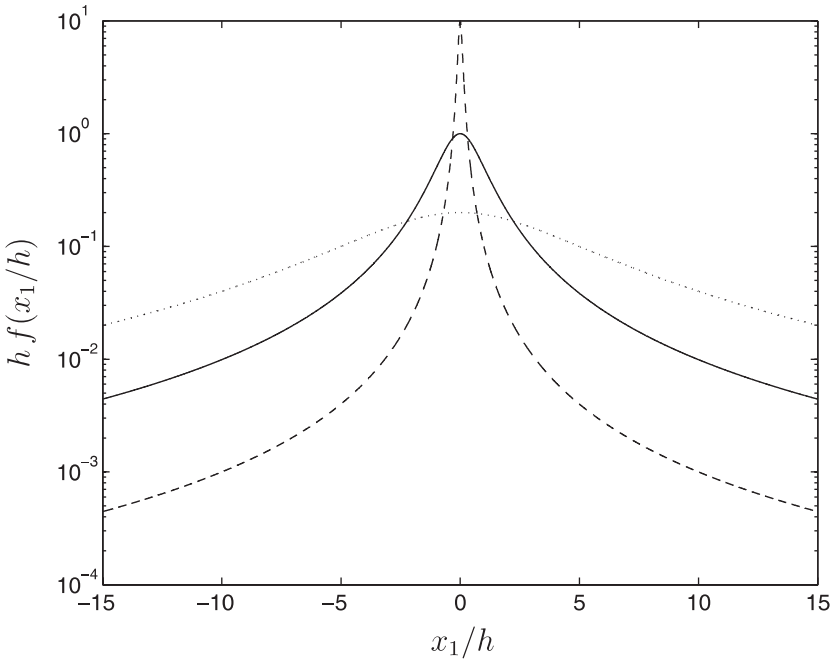

Fig. 2. "δ-type" force (8) normalised by half-thickness h; ——, $\beta = h$; − − −, $\beta = 0.1\,h$; ·····, $\beta = 5\,h$.

with inverse

$$g(x_1, x_3) = \frac{\Omega}{2\pi h}\int_{-\infty}^{+\infty} g_F(\alpha, x_3)\exp\left(\mathrm{i}\Omega\frac{x_1}{h}\alpha\right)\mathrm{d}\alpha, \tag{11}$$

where $g_F(\alpha, x_3)$ is the Fourier transform of the function $g(x_1, x_3)$, α is dimensionless Fourier transform parameter, $\Omega = \omega h/c_2^{(2)}$ is the dimensionless frequency.

For some combinations of problem parameters the function g_F possesses real poles. These may correspond to both Stoneley-type and Lamb-type waves. The existence of canonical interfacial Stoneley waves in a composite elastic half-space has been investigated by Cagniard [13]. The real poles associated with Lamb-type waves with a sinusoidal distribution along the thickness are only a feature of a "soft" interface. In the case of two real poles $\alpha = \pm\alpha_s$ the integration contour in (11) has to be deformed as it is shown in Fig. 3. As usual, the shape of a deformed contour is motivated by the radiation condition for harmonic waves with the time dependence $\exp(\mathrm{i}\,\omega\,t)$ taking into consideration the wave direction.

Applying transform (10) in Eqs. (3) and (4) and taking into account the radiation condition (9) we obtain

$$\phi_F^{(1)} = a_1^{(1)}\exp\left(-\Omega\xi_1^{(1)}\frac{|x_3|}{h}\right), \quad \psi_F^{(1)} = a_2^{(1)}\exp\left(-\Omega\xi_2^{(1)}\frac{|x_3|}{h}\right) \tag{12}$$

and

$$\begin{aligned}\phi_F^{(2)} &= a_1^{(2)}\left[\exp\left(-\Omega\xi_1^{(2)}\frac{x_3}{h}\right) + \exp\left(\Omega\xi_1^{(2)}\frac{x_3}{h}\right)\right],\\ \psi_F^{(2)} &= a_2^{(2)}\left[\exp\left(-\Omega\xi_2^{(2)}\frac{x_3}{h}\right) - \exp\left(\Omega\xi_2^{(2)}\frac{x_3}{h}\right)\right],\end{aligned} \tag{13}$$

where

$$\xi_1^{(1)} = \sqrt{\alpha^2 - \left(\frac{\kappa^{(1)}}{c_*}\right)^2}, \quad \xi_2^{(1)} = \sqrt{\alpha^2 - \frac{1}{c_*^2}},$$
$$\xi_1^{(2)} = \sqrt{\alpha^2 - (\kappa^{(2)})^2}, \quad \xi_2^{(2)} = \sqrt{\alpha^2 - 1}.$$

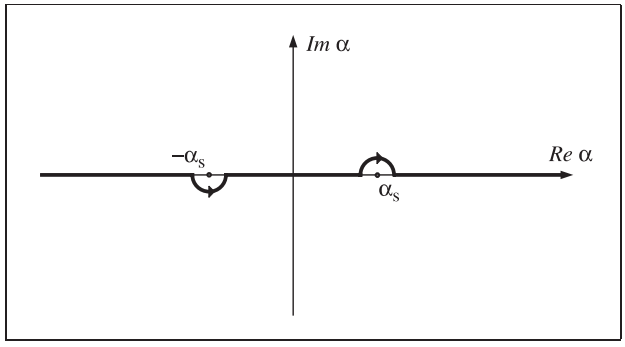

(a)

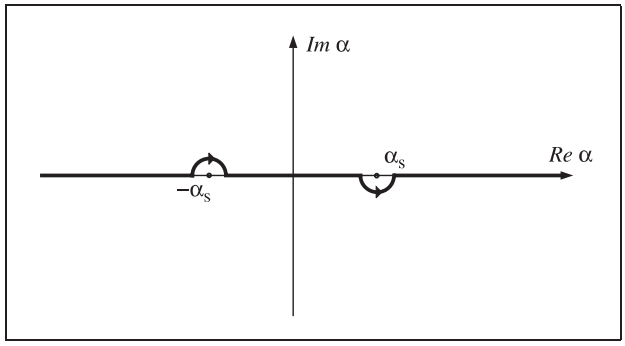

(b)

Fig. 3. Integration contour for inverse Fourier transform (11): (a) $x_1>0$; (b) $x_1<0$.

Here the branches of the functions $\xi_1^{(1)}$, $\xi_2^{(1)}$ and related branch cuts in the complex plane are chosen to satisfy the conditions $\sqrt{1}=1$ and $\sqrt{-1}=\mathrm{i}$.

The coefficients $a_j^{(i)}$, with $i,j=1,2$, in Eqs. (12) and (13) are found by applying the Fourier transform to the contact conditions (6) and (7). The Fourier transform of the function $f(x_1)$ in (8) is

$$\int_{-\infty}^{+\infty} f(x_1)\exp\left(-\mathrm{i}\Omega\frac{x_1}{h}\alpha\right)\mathrm{d}x_1=\exp\left(-\Omega|\alpha|\frac{\beta}{h}\right). \tag{14}$$

The right-hand side in Eq. (14) coincides with the transformed δ function ($\delta_F=1$) at $\beta=0$.

As a result, the exact solution of the problem is presented in the form of an integral (11). In particular, the transverse displacement at the interface $x_3=h$ can be written as

$$v_3(x_1,h)=\frac{A}{2\pi\rho^{(2)}(c_2^{(2)})^2}\int_{-\infty}^{+\infty} v_F(\alpha)\exp(\Omega(\mathrm{i}x_1\alpha-\beta|\alpha|)h^{-1})\,\mathrm{d}\alpha, \tag{15}$$

whereas the normal stress at the interface $x_3=h$ becomes

$$\sigma_{33}(x_1,h)=\frac{A\Omega}{2\pi h}\int_{-\infty}^{+\infty} \sigma_F(\alpha)\exp(\Omega(\mathrm{i}x_1\alpha-\beta|\alpha|)h^{-1})\,\mathrm{d}\alpha, \tag{16}$$

where

$$\begin{aligned} v_F(\alpha)=\gamma^{-1}\Big[&-S_1^{(2)}S_2^{(2)}(\alpha^2-\xi_1^{(1)}\xi_2^{(1)})\xi_1^{(2)}\\ &-\rho_*\xi_1^{(1)}(C_1^{(2)}S_2^{(2)}\alpha^2-C_2^{(2)}S_1^{(2)}\xi_1^{(2)}\xi_2^{(2)})\Big] \end{aligned} \tag{17}$$

and

$$\sigma_F(\alpha) = \gamma^{-1}\Big\{ C_1^{(2)} S_2^{(2)}(1-2\alpha^2) \times \Big[2\alpha^4(-1+\varepsilon c_*) - \xi_1^{(1)}\xi_2^{(1)} - \alpha^2(-1+\rho_*+2(-1+\varepsilon c_*)\xi_1^{(1)}\xi_2^{(1)})\Big] - C_2^{(2)} S_1^{(2)} 2\alpha^2 \Big[\rho_* - 2(-1+\varepsilon c_*)\alpha^2 + 2(-1+\varepsilon c_*)\xi_1^{(1)}\xi_2^{(1)}\Big]\xi_1^{(2)}\xi_2^{(2)} - \rho_* C_1^{(2)} C_2^{(2)} \xi_1^{(1)}\xi_2^{(2)}\Big\}, \tag{18}$$

with

$$\gamma = C_1^{(2)} S_2^{(2)}\Big\{-\alpha^2\big[-1+\rho_*-2(-1+\varepsilon c_*)\alpha^2\big]^2 + \big[1+2(-1+\varepsilon c_*)\alpha^2\big]^2 \xi_1^{(1)}\xi_2^{(1)}\Big\} + C_2^{(2)} S_1^{(2)}\Big\{\big[\rho_*-2(-1+\varepsilon c_*)\alpha^2\big]^2 - 4(-1+\varepsilon c_*)^2\alpha^2\xi_1^{(1)}\xi_2^{(1)}\Big\}\xi_1^{(2)}\xi_2^{(2)} + \rho_*\Big(S_1^{(2)}S_2^{(2)}\xi_2^{(1)}\xi_1^{(2)} + C_1^{(2)}C_2^{(2)}\xi_1^{(1)}\xi_2^{(2)}\Big), \tag{19}$$

where $S_1^{(2)} = \sinh(\Omega\xi_1^{(2)})$, $S_2^{(2)} = \sinh(\Omega\xi_2^{(2)})$, $C_1^{(2)} = \cosh(\Omega\xi_1^{(2)})$, $C_2^{(2)} = \cosh(\Omega\xi_2^{(2)})$.

The complicated Fourier integrals (15) and (16) do not allow for an immediate qualitative insight. This motivates a further asymptotic analysis of the original problem.

4. Thickness resonance frequencies

For the vertical interfacial excitation (7) we expect that the resonance phenomena of interest are related to thickness stretch vibrations. These are characterised by complex natural frequencies arising from the 1D problem for $\phi^{(i)}(x_3)$ (as before $i = 1, 2$):

$$\frac{\partial^2\phi^{(i)}}{\partial x_3^2} + \left(\frac{\omega}{c_1^{(i)}}\right)^2 \phi^{(i)} = 0, \tag{20}$$

with

$$\left.\frac{\partial\phi^{(1)}}{\partial x_3}\right|_{x_3=\pm h} = \left.\frac{\partial\phi^{(2)}}{\partial x_3}\right|_{x_3=\pm h} \tag{21}$$

and

$$\varepsilon\phi^{(1)}(\pm h) = c_*\phi^{(2)}(\pm h), \tag{22}$$

where

$$\frac{\partial\phi^{(1)}}{\partial x_3} + \mathrm{i}\frac{\omega}{c_1^{(1)}}\phi^{(1)} = 0. \tag{23}$$

The formulated problem follows from the relations in Section 2 at $\psi^{(i)} = \partial\phi^{(i)}/\partial x_1 = 0$ and $A = 0$. It governs stretch natural vibrations of a thin infinite fibre of the studied system (see Fig. 1).

For vibration modes symmetric in x_3, we have from the 1D equations (20) and the radiation condition (23) that

$$\phi^{(1)}(x_3) = C_1\exp\left(-\mathrm{i}\frac{\omega}{c_1^{(1)}}|x_3|\right), \quad \phi^{(2)}(x_3) = C_2\cos\left(\frac{\omega}{c_1^{(2)}}x_3\right), \tag{24}$$

where C_1 and C_2 are constants. By substituting these solutions into the contact conditions (21) and (22) we arrive at the transcendental equation

$$\kappa^{(1)}\cos(\kappa^{(2)}\Omega)+\mathrm{i}\varepsilon\kappa^{(2)}\sin(\kappa^{(2)}\Omega)=0. \tag{25}$$

Next, by using the complex decomposition $\Omega=\Omega_0+\mathrm{i}\Omega_1$ we have that

$$\begin{aligned}&\cos(\kappa^{(2)}\Omega_0)\left[\kappa^{(1)}\cosh(\kappa^{(2)}\Omega_1)-\varepsilon\kappa^{(2)}\sinh(\kappa^{(2)}\Omega_1)\right]\\&\quad+\mathrm{i}\,\sin\left(\kappa^{(2)}\Omega_0\right)\left[\varepsilon\kappa^{(2)}\cosh\left(\kappa^{(2)}\Omega_1\right)-\kappa^{(1)}\sinh\left(\kappa^{(2)}\Omega_1\right)\right]=0.\end{aligned} \tag{26}$$

The solution of the last equation becomes

$$\Omega_0=\Lambda_m^h,\quad \Omega_1=\frac{1}{\kappa^{(2)}}\tanh^{-1}\left(\frac{\varepsilon}{\varepsilon_0}\right)\quad\text{for } \varepsilon<\varepsilon_0 \tag{27}$$

and

$$\Omega_0=\Lambda_m^s,\quad \Omega_1=\frac{1}{\kappa^{(2)}}\coth^{-1}\left(\frac{\varepsilon}{\varepsilon_0}\right)\quad\text{for } \varepsilon>\varepsilon_0, \tag{28}$$

with $\Lambda_m^h=(\pi(2m-1))/2\kappa^{(2)}$, $\Lambda_m^s=\pi m/\kappa^{(2)}$, $m=1,2,\ldots$, and $\varepsilon_0=\kappa^{(1)}/\kappa^{(2)}$. In these formulae Λ_m^h and Λ_m^s denote thickness stretch resonance frequencies corresponding to the limiting cases of a layer with traction free ($\phi^{(2)}(\pm h)=0$) and fixed ($\mathrm{d}\phi^{(1)}/\mathrm{d}x_3|_{x_3=\pm h}=0$) faces, respectively (e.g. see Ref. [3]). The imaginary part Ω_1 is associated with the radiation to infinity and tends to zero for "hard" ($\varepsilon\ll1$) or "soft" ($\varepsilon\gg1$) layers. For the latter, we get from Eqs. (27) and (28), respectively

$$\Omega_1\approx\frac{1}{\kappa^{(1)}}\varepsilon\quad(\varepsilon\ll1) \tag{29}$$

and

$$\Omega_1\approx\frac{\kappa^{(1)}}{(\kappa^{(2)})^2\varepsilon}\quad(\varepsilon\gg1). \tag{30}$$

As it might be expected, we have from Eqs. (27) and (28)

$$\Omega_1\to\infty\quad\text{as}\quad\varepsilon\to\varepsilon_0. \tag{31}$$

In this case there is no reflection at the interfaces $x_3=\pm h$ (see also Fig. 4 illustrating the effect of the Poisson ratio on the imaginary part).

It is important to note that the denominator (19) of the Fourier transforms $v_F(\alpha)$ and $\sigma_F(\alpha)$ in Eqs. (17) and (18) has a double zero pole at $\alpha=0$ at the complex resonance frequencies given by formulae (27) and (28); hence the related Fourier integrals diverge.

5. An asymptotic analysis

In this section, we concentrate on two practically important cases corresponding to "hard" and "soft" interfacial layers. As we have already mentioned, for the latter the parameter ε in Eq. (1) may be assumed small or large, respectively.

5.1. "Hard" layer

A typical frequency dependence for small ε is displayed in Fig. 5. We clearly observe maxima near the frequencies Λ_m^h given by formula (27) which correspond to a layer with traction free faces. These frequencies are also characterised by wider peaks of the Fourier transform v_F near $\alpha=0$ (see Fig. 6). The numerical data in Figs. 5 and 6 agree with the consideration above. In fact, the relevant Fourier integrals become nearly divergent at the frequencies $\Omega=\Lambda_m^h$ when the imaginary part Ω_1 of complex stretch resonance frequencies practically vanishes (see estimation (29)). This is due to the long-wavelength contribution corresponding to small values of the parameter α. It should be noted that similar wide peaks may appear sometimes at

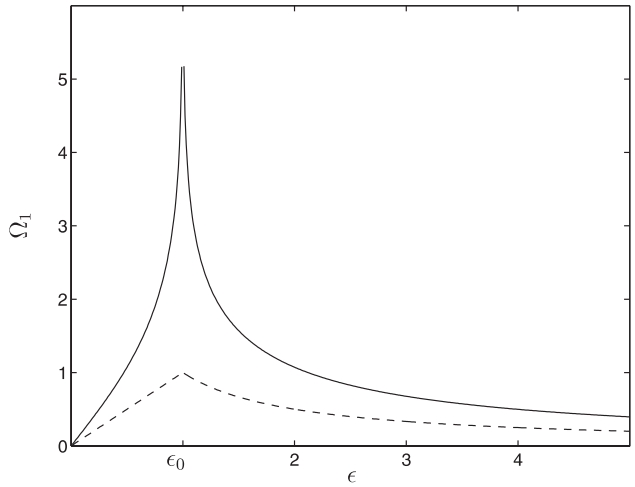

Fig. 4. Imaginary parts of thickness stretch resonance frequencies versus ε for $v^{(i)} = 0.3$ and $\varepsilon_0 = 1$; ——, Eq. (27) for $\varepsilon < \varepsilon_0$ and Eq. (28) for $\varepsilon > \varepsilon_0$; – – –, Eq. (29) for $\varepsilon < \varepsilon_0$ and Eq. (30) for $\varepsilon > \varepsilon_0$.

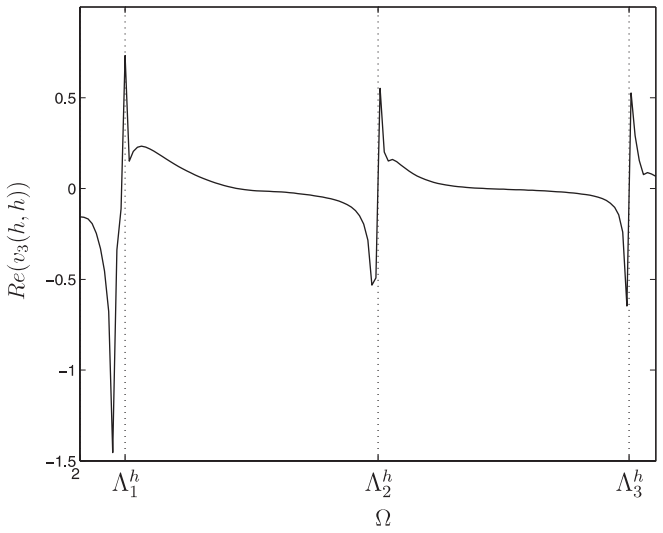

Fig. 5. Real part of transverse displacement at $x_1 = h$, $x_3 = h$ versus frequency for $v^{(i)} = 0.3$, $\rho_* = 0.1$, $c_* = 0.1$.

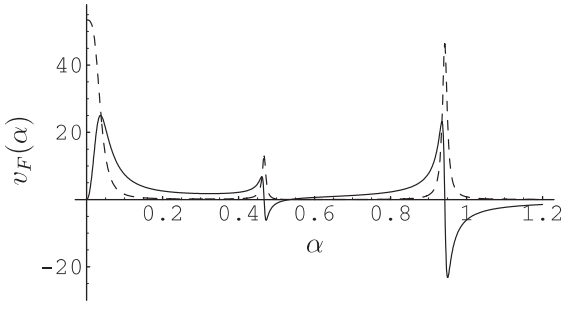

Fig. 6. Fourier transform (17) at $\Omega = \Lambda_1^h$ for $v^{(i)} = 0.3$, $\rho_* = 0.1$, $c_* = 0.1$; ——, real part; – – –, imaginary part.

none-zero values of the parameter α. These are also a feature of a fluid-loaded layer (e.g. see Ref. [9]) and usually correspond to "non-regular" cut-offs that are not related to thickness resonance phenomena (see Ref. [14] for more details).

Next, we specify the vicinities of the thickness resonance frequencies corresponding to a layer with traction free faces as $\Omega = \Lambda_m^h + \eta$, where $\eta \sim \varepsilon$. Then, neglecting secondary terms in the formula (17) at $\alpha \sim \varepsilon^{1/2}$ we get $v_F(\alpha) = v_F^0(\alpha) + \ldots$, where

$$v_F^0(\alpha) = \frac{-1 + (-\eta + \mathrm{i}\varepsilon)\cot(\Lambda_m^h)}{-\eta + \mathrm{i}\varepsilon/\kappa^{(1)} + 1/2\alpha^2 T_h \Lambda_m^h} + \ldots, \tag{32}$$

with

$$T_h = \frac{1}{(\kappa^{(2)})^2}\left[1 + \frac{8(\kappa^{(2)})^2 \cot(\Lambda_m^h)}{\Lambda_m^h}\right]. \tag{33}$$

The denominator of the Fourier transform $v_F^0(\alpha)$ in formula (32) has the double zero pole $\alpha = 0$ at the value $\eta = \mathrm{i}\varepsilon/\kappa^{(1)}$ corresponding to the complex resonance frequencies (27) with the imaginary part approximated by the formula (29) oriented to small ε. As was stated above, the presence of the latter is caused by the radiation into a softer environment.

By substituting the asymptotic behaviour (32) into the Fourier integral (15) and calculating the residues for small complex poles of order $O(\varepsilon^{1/2})$ we get $v_3(x_1) = v_3^0(x_1) + \ldots$, where

$$v_3^0(x_1) = \frac{A}{\rho^{(2)}(c_2^{(2)})^2} \frac{\mathrm{i}\exp(\Lambda_m^h(\mathrm{i}x_1\alpha_h - \beta|\alpha_h|)h^{-1})}{\alpha_h T_h \Lambda_m^h}[-1 + (-\eta + \mathrm{i}\varepsilon)\cot(\Lambda_m^h)], \tag{34}$$

with

$$\alpha_h = \sqrt{\frac{2(\eta - \mathrm{i}\varepsilon/\kappa^{(1)})}{T_h \Lambda_m^h}}.$$

It is remarkable that the asymptotic formula (34) might be immediately derived starting from the 1D asymptotic model describing high-frequency long-wavelength motions of a "hard" layer radiating into the environment. This model represents a perturbation in ε to that for a layer with traction free faces (e.g. see Ref. [3] for more detail) and is governed by the equation

$$\frac{T_h h^2}{2\Lambda_m^h}\frac{\partial^2 v_3^0}{\partial x_1^2} + \left(\eta - \frac{\mathrm{i}\varepsilon}{\kappa^{(1)}}\right)v_3^0 = \frac{hAf(x_1)}{\Lambda_m^h \rho^{(2)}(c_2^{(2)})^2}[1 + (\eta - \mathrm{i}\varepsilon)\cot(\Lambda_m^h)], \tag{35}$$

written in terms of the long-wavelength amplitude v_3^0 of thickness stretch vibrations. It can be easily verified that the solution to this equation takes the form (34).

In conclusion, we mention that the case considered in this sub-section is similar to that of a plate under a light fluid loading (see Ref. [9]). The point is that "extra" shear waves characteristic of an elastic environment do not affect considerably the stretch vibrations of interest.

5.2. "Soft" layer

For a "soft" interfacial layer, $\varepsilon \gg 1$, we concentrate on the vicinities of the thickness stretch resonance frequencies (28) corresponding to a layer with fixed faces (see also Fig. 7 displaying a Fourier transform (18) for the interfacial stress characteristic of this case). Now, the parameter α is assumed to be $\alpha \sim \varepsilon^{-1/2}$ and the frequency Ω may be expressed as $\Omega = \Lambda_m^h + \eta$. Thus, we get from the formula (18) $\sigma_F(\alpha) = \sigma_F^0(\alpha) + \ldots$, where

$$\sigma_F^0(\alpha) = \frac{\mathrm{i}/\varepsilon[1 + (-\eta + \mathrm{i}/\varepsilon)\tan(\Lambda_m^s)]}{\eta(\kappa^{(2)})^2/\kappa^{(1)} - \mathrm{i}/\varepsilon - 1/2\alpha^2 T_s \Lambda_m^s} + \ldots, \tag{36}$$

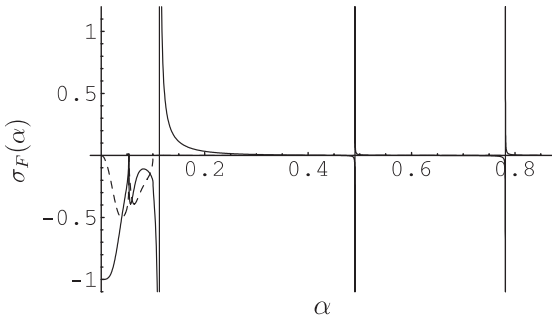

Fig. 7. Fourier transform (18) at $\Omega = \Lambda_1^s$ for $\nu^{(i)} = 0.3$, $\rho_* = 10$, $c_* = 10$; ——, real part; − − −, imaginary part.

with

$$T_s = \frac{1}{\kappa^{(1)}}\left[1 - \frac{2\tan(\Lambda_m^s)}{\Lambda_m^s}\right]. \tag{37}$$

The denominator here is related to the complex thickness resonance frequencies of a layer enclosed into a harder environment (see Eq. (30)).

Finally, we have $\sigma_{33}(x_1) = \sigma_{33}^0(x_1) + \ldots$, where

$$\sigma_{33}^0(x_1) = \frac{A\Omega}{h\varepsilon}\frac{\exp(\Lambda_m^s(\mathrm{i}x_1\alpha_s - \beta|\alpha_s|)h^{-1})}{\alpha_s T_s \Lambda_m^s}[1 + (-\eta + \mathrm{i}/\varepsilon)\tan(\Lambda_m^s)], \tag{38}$$

with

$$\alpha_s = \sqrt{\frac{2[\eta(\kappa^{(2)})^2/\kappa^{(1)} - \mathrm{i}/\varepsilon]}{T_s\Lambda_m^s}}.$$

The associated high-frequency long-wavelength equation becomes

$$\frac{T_s h^2}{2\Lambda_m^s}\frac{\partial^2\sigma_{33}^0}{\partial x_1^2} + \left[\eta\frac{(\kappa^{(2)})^2}{\kappa^{(1)}} - \frac{\mathrm{i}}{\varepsilon}\right]\sigma_{33}^0 = \frac{\mathrm{i}Af(x_1)}{\varepsilon}\left[1 - \left(\eta - \frac{\mathrm{i}}{\varepsilon}\right)\tan(\Lambda_m^s)\right]. \tag{39}$$

In the limit $\varepsilon \to \infty$ it transforms to that for a layer with fixed faces (see Refs. [10,3]).

6. Numerical comparison

First, we compare the exact Fourier transforms $v_F(\alpha)$ and $\sigma_F(\alpha)$ and their asymptotic analogues $v_F^0(\alpha)$ and $\sigma_F^0(\alpha)$, both calculated at the thickness resonance frequencies Λ_1^h and Λ_1^s, which correspond to "hard" and "soft" interfacial layers, respectively. Here, and below, we use the Poisson ratio $\nu^{(i)} = 0.3$ $(i = 1, 2)$. The graphs in Figs. 8 and 9 demonstrate the efficiency of the asymptotics over the long-wavelength region ($\alpha \ll 1$). The sharp bend at $\alpha \approx 0.05$ in Fig. 9 corresponds to the branch point $\alpha = \kappa^{(1)}/c_*$ of $\xi_1^{(1)}$ which is outside of the validity range of the long-wavelength asymptotics.

Typical resonant curves and spatial distributions of displacements and stresses are presented in Figs. 10–13 for the "δ-type" force (8) with $\beta = h$. All the displayed displacements and stresses are normalised by $A/(\pi\rho^{(2)}(c_2^{(2)})^2)$ and $A\Omega/\pi h$, respectively. The frequency dependences near the first limiting stretch resonance frequencies Λ_1^h and Λ_1^s are demonstrated in Figs. 10 and 11. Figs. 12 and 13 illustrate resonance motions of the interface $x_3 = h$. These are characterised by oscillating of the exact solution around the asymptotic ones. The small superimposed short-wavelength oscillations cannot be captured by the proposed theory. All the figures confirm the basic assumption regarding the major contribution of long-wavelength components near thickness resonance frequencies. Thus, the use of the 1D models for "hard" and "soft" interfacial layers seems to be justified.

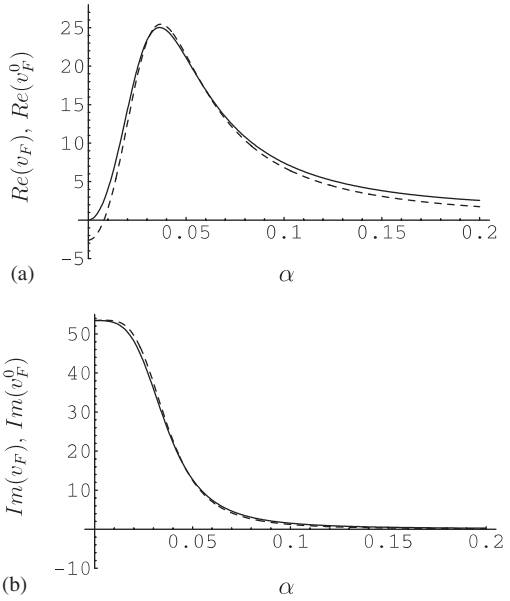

Fig. 8. Approximation of transformed displacement at $\Omega = \Lambda_1^h$ for $\rho_* = 0.1$, $c_* = 0.1$; ——, v_F by Eq. (17); – – –, v_F^0 by Eq. (32): (a) real part; (b) imaginary part.

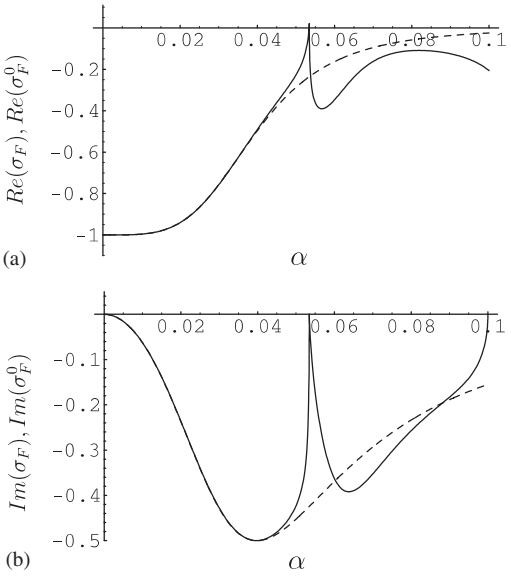

Fig. 9. Approximation of transformed normal stress at $\Omega = \Lambda_1^s$ for $\rho_* = 10$, $c_* = 10$; ——, σ_F by Eq. (18); – – –, σ_F^0 by Eq. (36): (a) real part; (b) imaginary part.

Numerical results for an interfacial layer with a relative impedance $\varepsilon = \varepsilon_0$ (see Eq. (31)) are presented in Fig. 14. It is evident that such a layer cannot be treated either as a "hard" or as a "soft" one. The transverse displacement is calculated by Eq. (15) with the same normalisation as before. As might be expected, we do not observe now (see Fig. 14(a)) typical peaks in the vicinity of the frequencies Λ_m^h similar to those in Figs. 5 and 10 for a "hard" layer. In this case the imaginary part of thickness stretch resonance frequencies tends to infinity (see Eq. (31)) and resonance vibrations are suppressed.

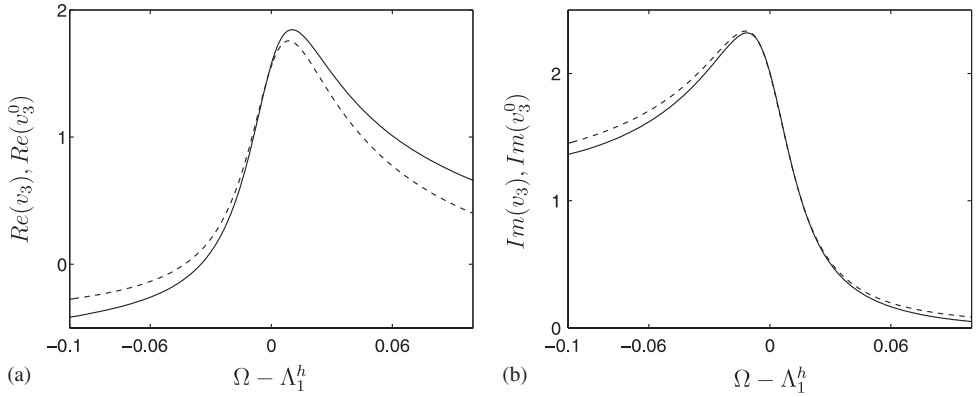

Fig. 10. Transverse displacement $v_3(h,h)$ near first thickness stretch resonance frequency $\Omega = \Lambda_1^h$ for $\rho_* = 0.1$, $c_* = 0.1$, $\beta = h$; ——, exact solution (15); – – –, asymptotic solution (34): (a) real part; (b) imaginary part.

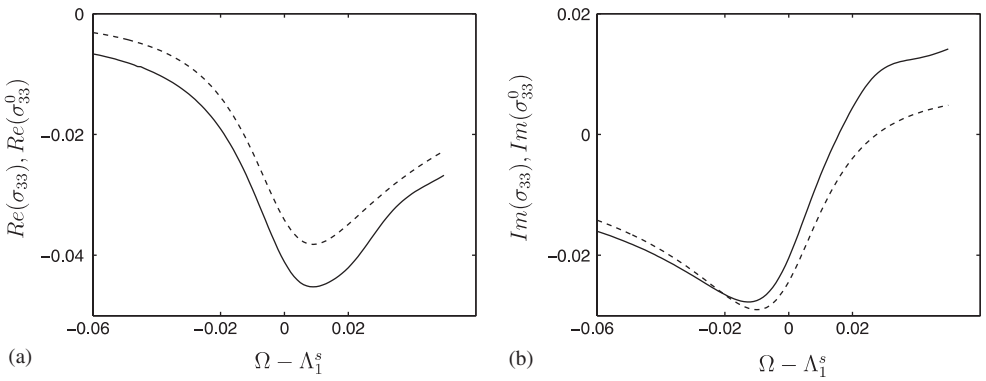

Fig. 11. Normal stress $\sigma_3(h,h)$ near first thickness stretch resonance frequency $\Omega = \Lambda_1^s$ for $\rho_* = 10$, $c_* = 10$, $\beta = h$; ——, exact solution (16); – – –, asymptotic solution (38): (a) real part; (b) imaginary part.

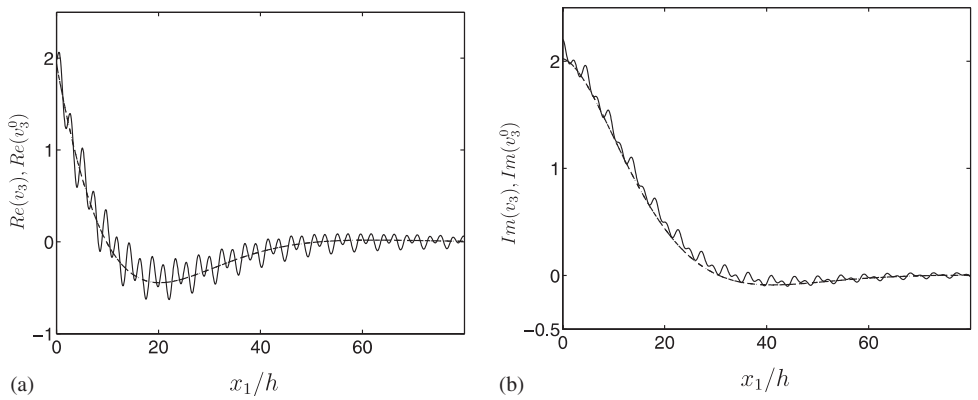

Fig. 12. Transverse displacements of interface $x_3 = h$ at $\Omega = \Lambda_1^h$ for $\rho_* = 0.1$, $c_* = 0.1$, $\beta = h$; ——, exact solution (15); – – –, asymptotic solution (34): (a) real part; (b) imaginary part.

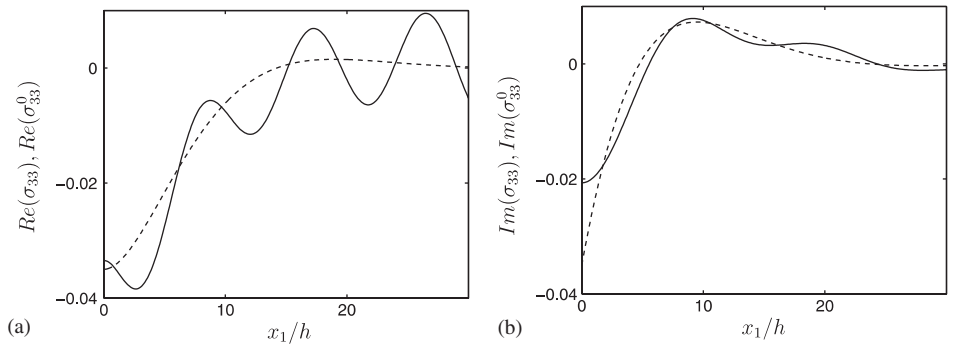

Fig. 13. Normal stress $\sigma_3(x_1, h)$ of interface $x_3 = h$ at $\Omega = \Lambda_1^s$ for $\rho_* = 10$, $c_* = 10$, $\beta = h$; ——, exact solution (16); − − −, asymptotic solution (38): (a) real part; (b) imaginary part.

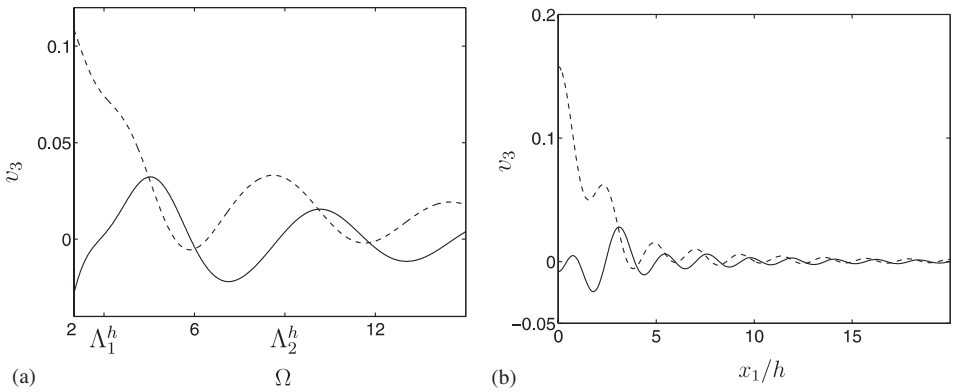

Fig. 14. Interfacial layer with $\rho_* = 1$, $c_* = 1$, $\beta = h$; ——, real part of (15); − − −, imaginary part of (15): (a) transverse displacement at $x_1 = h, x_3 = h$ versus frequency; (b) transverse displacements of interface $x_3 = h$ at first thickness stretch resonance frequency $\Omega = \Lambda_1^h$.

Finally, we study the effect of the parameter β in Eq. (8) that characterises the distribution of external forces. The transverse displacements of the interfacial layer are plotted in Figs. 15(a)–(b) for $\beta = 0.1h$ and $5h$, respectively. It is clear that the effect of small amplitude short-wavelength oscillations is greater if the force (8) is close to the δ-function. Hence, the efficiency of the proposed long-wavelength asymptotics is higher for distributed loads, when the parameter β takes larger values, because of the dominant contribution of related modes.

7. Concluding remarks

The developed theory of interfacial thickness vibrations is not restricted to the case of a flat infinite layer presented in the paper. The 1D long-wavelength high-frequency approximations (35) and (39) have a potential for various extensions to more complicated geometries, constitutive relations and contact conditions.

The elementary formulae in Section 4 for complex stretch resonance frequencies represent an important quantitative characteristic of interfacial dynamic behaviour. In particular, they may be useful for evaluating the accuracy of the approximation of a "soft"/"hard" layer tending to the limit of a layer with traction free/fixed faces.

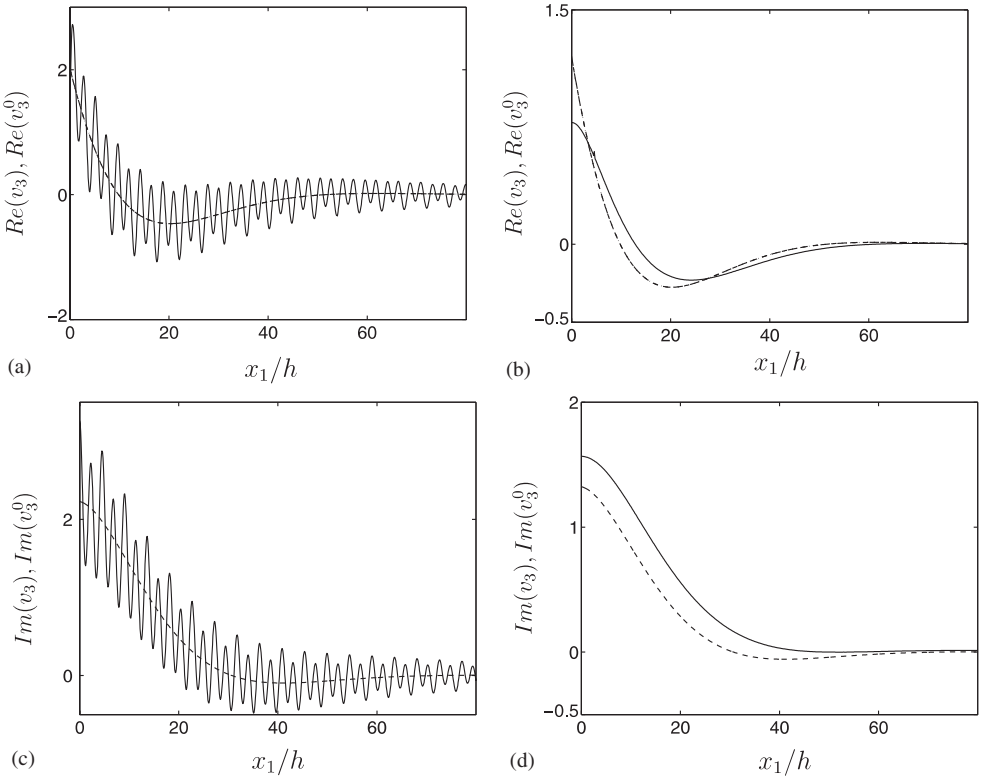

Fig. 15. Displacements of interface $x_3 = h$ induced by "δ-type" force (8); for $\rho_* = 0.1$, $c_* = 0.1$, $\Omega = \Lambda_1^h$; ——, exact solution (15); – – –, asymptotic solution (34): (a) real part for $\beta = 0.1h$; (b) real part for $\beta = 5h$; (c) imaginary part for $\beta = 0.1h$; (d) imaginary part for $\beta = 5h$.

Acknowledgements

The work of the second author is supported by the UK Overseas Research Student Award, the University of Manchester and the University of Brunel. These awards are very gratefully acknowledged. The authors are also grateful to referees for valuable comments.

References

[1] L.M. Brekhovskikh, *Waves in Layered Media*, Academic Press, Orlando, 1980.
[2] W.M. Ewing, W.S. Jardetzky, *Elastic Waves in Layered Media*, McGraw-Hill, New York, 1957.
[3] J.D. Kaplunov, L.Yu. Kossovich, E.V. Nolde, *Dynamics of Thin Walled Elastic Bodies*, Academic Press, San Diego, 1998.
[4] N.D. Veksler, *Acoustic Spectroscopy*, Springer, Berlin, 1993.
[5] C.C.H. Guyott, P. Cawley, The ultrasonic vibration characteristics of adhesive joints, *Journal of the Acoustical Society of America* 83 (1988) 632–640.
[6] M.J.S. Lowe, P. Cawley, Comparison of the modal properties of a stiff layer embedded in a solid medium with the minima of the plane-wave reflection coefficient, *Journal of the Acoustical Society of America* 97 (1995) 1625–1637.
[7] A.I. Lavrentyev, S.I. Rokhlin, Ultrasonic study of environmental damage initiation and evolution in adhesive joints, *Research in Nondestructive Evaluation* 10 (1998) 17–41.
[8] A.I. Lavrentyev, S.I. Rokhlin, An ultrasonic method for determination of elastic moduli, density, attenuation and thickness of a polymer coating on stiff plate, *Ultrasonics* 39 (2001) 211–221.
[9] J.D. Kaplunov, D.G. Markushevich, Plane vibrations and radiation of an elastic layer lying on liquid half-space, *Wave Motion* 17 (1993) 199–211.
[10] J.D. Kaplunov, Long wave vibrations of a thin-walled body with fixed faces, *The Quarterly Journal of Mechanics and Applied Mathematics* 48 (1995) 311–327.

[11] G.C. Gaunaurd, Elastic and acoustic resonance wave scattering, *Applied Mechanics Reviews* 42 (1989) 143–192.
[12] J.D. Achenbach, *Wave Propagation in Elastic Solids*, Elsevier Science Publisher B.V., New York, 1984.
[13] L. Cagniard, *Reflection and Refraction of Progressive Seismic Waves*, McGraw-Hill, New York, 1962.
[14] R.D. Gregory, I. Gladwell, The reflection of a symmetric Rayleigh–Lamb wave at the fixed or free edge of a plate, *Journal of Elasticity* 13 (1983) 185–206.